Data-Driven Fingerprint Reconstruction from Minutiae Based on Real and Synthetic Training Data

Andrey Makrushin, Venkata Srinath Mannam and Jana Dittmann
Department of Computer Science, Otto von Guericke University, Universitaetsplatz 2, 39106 Magdeburg, Germany

Keywords: Fingerprint Reconstruction, Minutiae Map, GAN, Pix2pix.

Abstract: Fingerprint reconstruction from minutiae performed by model-based approaches often lead to fingerprint patterns that lack realism. In contrast, data-driven reconstruction leads to realistic fingerprints, but the reproduction of a fingerprint's identity remain a challenging problem. In this paper, we examine the pix2pix network to fit for the reconstruction of realistic high-quality fingerprint images from minutiae maps. For encoding minutiae in minutiae maps we propose *directed line* and *pointing minutiae* approaches. We extend the pix2pix architecture to process complete plain fingerprints at their native resolution. Although our focus is on biometric fingerprints, the same concept fits for synthesis of latent fingerprints. We train models based on real and synthetic datasets and compare their performances regarding realistic appearance of generated fingerprints and reconstruction success. Our experiments establish pix2pix to be a valid and scalable solution. Reconstruction from minutiae enables identity-aware generation of synthetic fingerprints which in turn enables compilation of large-scale privacy-friendly synthetic fingerprint datasets including mated impressions.

1 INTRODUCTION

Fingerprint is a widely accepted and broadly used means of biometric user authentication. Applications making use of fingerprint authentication range from unlocking mobile phones to access control to financial and governmental services. Hence, further development and continuous improvement of fingerprint matching systems cannot be overrated. The validity of fingerprint processing and matching algorithms is assessed empirically in experiments with large-scale fingerprint datasets. Taking into account the current trend of using machine learning and in particular deep convolutional neural networks, an abundant amount of training and validation samples is an indispensable part of the development process.

Recent cross-border regulations on protection of private data are a hurdle that make usage of real biometric datasets difficult. For instance, the article 9 of the EU General Data Protection Regulation (GDPR) prohibits processing of biometric data for the purpose of uniquely identifying a natural person, however with some exceptions. In general, biometric data are seen as a special case of private data implying that collection, processing and sharing of such data are under strong regulation. Many biometric datasets have been recently removed from the public access due to possible conflicts with regulations. The prominent examples are the NIST fingerprint datasets SD4, SD14 and SD27. The documentation of the new NIST fingerprint dataset SD300 confirms that all subjects whose biometrics appear in the dataset are deceased (https://www.nist.gov/itl/iad/image-group/nist-special-database-300). A straightforward way to overcome the restrictions is introduction of virtual individuals and synthesis of biometric samples which belong to them. The synthetic fingerprints should possess the same characteristics as real ones, but it should be impossible to link them to any natural person.

Fingerprint synthesis is a special case of realistic image synthesis that has recently been solved by generative adversarial networks (GAN). Generation of random realistic fingerprints which inherit visual characteristics of fingerprints in a training dataset is not challenging looking at the current state of technologies. For instance, the established NVIDIA GAN architectures such as StyleGAN (Karras et al. 2018) can easily be trained to solve this task (Seidlitz et al. 2021 and Bahmani et al. 2021). The challenging part is synthesis of mated impressions which requires identity-aware conditional generation and a mechanism for simulating intra-class variations.

Based on the fact that the majority of algorithms rely on minutiae for fingerprint matching, it can be stated that the fingerprint identity is de facto given

Makrushin, A., Mannam, V. and Dittmann, J.
Data-Driven Fingerprint Reconstruction from Minutiae Based on Real and Synthetic Training Data.
DOI: 10.5220/0011660800003417
In *Proceedings of the 18th International Joint Conference on Computer Vision, Imaging and Computer Graphics Theory and Applications (VISIGRAPP 2023) - Volume 4: VISAPP*, pages 229-237
ISBN: 978-989-758-634-7; ISSN: 2184-4321

by minutiae co-allocation. Minutiae are the local characteristics of fingerprint ridges e.g. bifurcations where a line splits up into two or terminations where a line ends. A list of extracted minutiae is referred to as minutiae template. There are several standards describing the structure of a minutiae template e.g. ISO/IEC 19794-2:2011 or ANSI INCITS 381-2004.

Hence, the straightforward way to control the identity of synthetic fingerprints is reconstruction from a minutiae template. On the one hand, reconstruction from minutiae is clearly an ill-posed problem, on the other hand, minutiae locations reveal information about the ridge flow so that a reconstructed fingerprint has both minutiae at correct locations and a proper basic pattern. Note that reconstruction from pseudo-random minutiae helps to fulfill requirements on anonymity and diversity of synthetic fingerprints (Makrushin et al. 2021) and also enables synthesis of mated impressions.

As stated in (Mistry et al. 2020), fingerprints reconstructed from minutiae based on mathematical modeling lack realism. Recently, realistic fingerprints have been reconstructed by applying conditional GAN (Makrushin et al. 2022, Bouzaglo and Keller 2022 and Wijewardena et al. 2022). Although the identity control is a challenging part of such a data-driven approach, it has been demonstrated that the vast majority of reconstructed fingerprints match the reference fingerprints.

Here, we further investigate the application of the pix2pix network (Isola et al. 2017) to fingerprint reconstruction from minutiae focusing on 512x512 pixel images with an optical resolution of 500 ppi. Both, the generator and discriminator of the original network are extended by one convolutional layer to handle the aforementioned image size. Motivated by (Kim et al. 2019, Makrushin et al. 2022 and Bouzaglo and Keller 2022) we explore several minutiae encoding schemes for the optimal reconstruction. Last but not least, we train the reconstruction (generative) models not only from real but also from realistic synthetic fingerprints to figure out the suitability of our previously generated synthetic dataset for this task. Since visual characteristics of GAN-synthesized fingerprints are inherited from training samples, such a synthesis approach is applicable not only for biometric (plain) or forensic (latent) fingerprints but also for style transfer: plain to latent or latent to plain.

Our contribution can be summarized as follows:

- Modification of the pix2pix architecture to process 512x512 pixel images
- Introduction of a dataset of 50k synthetic fingerprints generated by our StyleGAN2-ada model trained from the Neurotechnology CrossMatch fingerprint dataset
- Training of pix2pix models from real and synthetic datasets with two different types of minutiae encoding: *directed line* and *pointing minutiae*
- Comparing *synthetic* and *real* datasets for the purpose of training pix2pix models
- Comparing *directed line* and *pointing minutiae* encoding approaches

Hereafter, the paper is organized as follows: Section 2 outlines the related work. Section 3 introduces our concept of applying pix2pix to fingerprint reconstruction. Training of our generative models is described in Section 4. Our experiments are in Section 5. Section 6 concludes the paper with the summary of results.

2 RELATED WORK

2.1 Model-Based Reconstruction

The de facto state-of-the-art approach to model-based fingerprint synthesis is implemented in the commercial tool SFinGe (Cappelli 2009). In order to create realistic patterns the physical characteristics of fingers, the contact between finger and the sensor surface as well as sensor characteristics are simulated. An open source implementation of a model-based fingerprint generator similar to SFinGe is called Anguli (Ansari 2011) and is available at https://dsl.cds.iisc.ac.in/projects/Anguli/.

The most prominent study on inversion of fingerprint templates is (Cappelli et al. 2007). Based on the zero-pole model (Sherlock and Monro 1993), the locations of singular points are estimated from the given minutiae followed by estimation of orientation and ridge frequency maps. Alternatively, ridge patterns can be reconstructed using the minutiae triplet model (Ross et al. 2007) or the AM-FM model (Feng and Jain 2009 and Li and Kot 2012) which makes use of eight neighbouring minutiae. An approach proposed in (Cao and Jain 2015) reconstructs ridge patterns based on patch dictionaries which allows for generating idealistic ridge patterns clearly lacking realism.

2.2 Data-Driven Reconstruction

Recently, fingerprint synthesis using GAN or a combination of GAN and autoencoder has become a trend. An identity-aware synthesis requires, however, a conditional GAN in which the network is guided to generate specific data by conditioning over some meaningful information rather than feeding a random latent vector as proposed in the original GAN.

As originally shown in (Kim et al. 2019) the task of fingerprint reconstruction from minutiae can be replaced by the image-to-image translation so that minutiae points are drawn on an image called minutiae map and then the minutiae map is translated to a fingerprint image. The original pix2pix network has been applied as one delivering state-of-the-art results in image-to-image translation. The experiments are conducted with an in-house fingerprint database. The generalization ability of pix2pix in application to fingerprint reconstruction from minutiae is challenged in (Makrushin et al. 2022) by conducting cross-sensor and cross-dataset experiments. The major limitation of the original pix2pix is that it is tuned to process images of 256x256 pixels or lower. The pix2pixHD extension (Wang et al. 2018) is a cumbersome solution to process larger images.

In (Bouzaglo and Keller 2022) a convolutional minutiae-to-vector encoder is used in combination with StyleGAN2 (Karras et al. 2019) for identity-preserving, attributes-aware fingerprint reconstruction from minutiae. The study in (Wijewardena et al. 2022) extends fingerprint reconstruction from minutiae to reconstruction from deep network embeddings. The inversion attack performances of both reconstruction schemes are evaluated and compared qualitatively and quantitatively.

To the best of our knowledge, in none of studies on data-driven fingerprint reconstruction the generative models are trained based on synthetic samples.

3 OUR CONCEPT

Let I be a fingerprint image and $L : L_i = (x_i, y_i, t_i, \theta_i)$ be a set of minutiae where (x_i, y_i) is a location of the i-th minutiae, t_i is a type (either bifurcation or ending) and θ_i is a direction. Our task is to train a conditional GAN that is capable of generating a fingerprint image I^* from L. The resulting synthetic fingerprint I^* should appear realistic and be biometrically as similar as possible to the original fingerprint I.

3.1 Minutiae Encoding

Construction of a minutiae map is visualized in Figure 1. It starts with minutiae extraction which can be done with an arbitrary tool. We use Neurotechnology VeriFinger SDK v12.0 (https://www.neurotechnology.com/verifinger.html). Next, the resulting list of minutiae is encoded into a minutiae map. We address three encoding schemes: encoding by gray squares, by directed lines and by pointing minutiae.

Gray Squares. Encoding minutiae by gray squares is originally proposed in (Kim et al. 2019). For each minutiae L_i from the minutiae list L a gray square of a fixed size is drawn with a center at (x_i, y_i). The shade of gray encodes the minutiae angle θ_i. In order to differentiate between endings and bifurcations, we use colors from 0 to 127 to quantize the directions of endings and colors from 129 to 255 to quantize the directions of bifurcations. The background color of a minutiae map is set to 128. For 500 ppi fingerprints depicted on 512x512 pixel images, the square size is set to 13x13.

Directed Lines. As proposed in (Makrushin et al. 2022) each minutiae L_i from the minutiae list L is encoded by a directed line which starts at (x_i, y_i) and is drawn to the direction given by the angle θ_i. Bifurcations are encoded by white lines (color=255) and endings by black lines (color=0). The background color is set to 128. It is stated that such a color selection emphasizes the dualism of bifurcations and endings and the directed line encoding is superior to a gray square encoding. It is also stated that shades of gray used as direction encoding may dilute during convolutions. For 500 ppi fingerprints, we set the line length to 15 pixels and the line width to 4 pixels.

Pointing Minutiae. The idea of using pointing minutiae is derived from (Bouzaglo and Keller 2022). We define a pointing minutiae as a combination of a square centered at (x_i, y_i) and a line pointing in the minutiae direction θ_i. Similar to directed line encoding, bifurcations are encoded by white lines (color=255) and endings by black lines (color=0). The background color is set to 128. Directed line and pointing minutiae encoding schemes perfectly reflect the complimentary nature of endings and bifurcations and therefore are robust to color inversion. For 500 ppi fingerprints the line length is set to 15 pixels, the line width to 4 pixels and the square size to 7x7 pixels.

3.2 Pix2pix Architecture

The pix2pix network (Isola et al. 2017) applied in our experiments is a conditional GAN consisting of generator and discriminator networks which are trained in an adversarial manner. The generator produces realistic images while the discriminator tells synthetic and real images apart. In our setup, the generator translates a minutiae map into a fingerprint image and the discriminator makes a decision for a tensor made of a fingerprint image and a minutiae map which is taken as a condition. After training is finished, we make no use of the discriminator and the generator is used for fingerprint reconstruction.

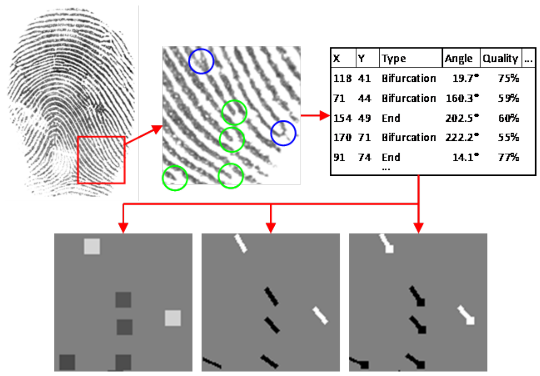

Figure 1: Minutiae map construction: minutiae extraction followed by minutiae encoding (gray squares, directed lines and pointing minutiae).

The original pix2pix architecture is designed for 256x256 pixel images which would require downscaling of a fingerprint image to make a complete fingerprint fit into it. In order to support a fingerprint-native resolution of 500 ppi and enable training with images of 512x512 pixels, we extend both generator and discriminator by one convolutional layer.

Generator. The generator architecture is based on the U-Net originally proposed in (Ronneberger et al. 2015). In contrast to other approaches based on encoder-decoder architecture used for solving the image-to-image translation problem, the U-Net pass information via skip connections to subsequent parallel layers as shown in the Figure 2. Indeed, the standard encoder-decoder networks first gradually down-sample a given input at each layer into a compressed representation called bottleneck and then gradually up-sample from the bottleneck at each layer to the original size. Hence, such networks fully rely on the bottleneck layer implying that it preserves all the information about the input. If it is not the case, the reconstructed image might miss important details.

Discriminator.The convolutional patch-based discriminator utilized in pix2pix classifies the given input as synthetic or real at a patch level. It means that the the network simultaneously makes a decision for each image patch and the final decision is a majority voting over all patches. The discriminator is a series of convolution layers with an input of shape *LxL* and the output of shape *RxR*. Each neuron at *RxR* classifies a single portion in *LxL*. The value of *L* at the network input layer is set to 512 and the value of *R* at the network output layer is 30 as in the original PatchGAN. A discriminator with a focus on single patch classification is shown in Figure 3. Even though the code is not explicitly written in a way to work at patch level it happens implicitly due to the nature of a convolution operation. In contrast to the original work where the receptive field (patch) size is 70x70 pixels, the addition of a convolutional layer has led to the enlargement of the receptive field to 142x142 pixels. It can be thought as 142x142 patch convolves over the given input image 30 times in each direction so that each 142x142 patch of an input image is classified by the corresponding bit in a 30x30 output. Finally the majority voting is done for 900 single patch votes. Note that the input of the discriminator is a tensor comprised of the minutiae map given to the generator and the real or synthetic fingerprint. It is justified that low frequencies can be captured by L1 loss and an improvement is needed for capturing variations at high-frequencies.

3.3 Training Datasets

The focus of this work is on generation of *realistic plain biometric* fingerprints. Hence, for training our generative models we selected high fidelity plain fingerprints captured by optical biometric sensors such as Cross Match Verifier 300. Our training dataset is comprised of:

- The Neurotechnology CrossMatch dataset that includes 408 samples and is provided on https://www.neurotechnology.com/download.html
- The DB1 A+B dataset used for the Second International Fingerprint Verification Competition (FVC2002) that includes 880 samples, http://bias.csr.unibo.it/fvc2002/databases.asp
- The DB1 A+B dataset used for the Third International Fingerprint Verification Competition (FVC2004) that also includes 880 samples, http://bias.csr.unibo.it/fvc2004/databases.asp

Note that images in the FVC2002 DB1 A+B have been collected with the TouchView II scanner by Identix. The total number of samples is 2168.

Since, the selection of training data is the only factor that predetermines the appearance of reconstructed fingerprints, our concept can be equally well applied to reconstitution of forensic fingerprints by using a dataset of exemplars or latents for training.

Data Augmentation is performed aiming at increasing the amount of training data as well as its variability. We horizontally flip and rotate images with eight rotation angles: +/-5°, +/-10°, +/-15°and +/-20°. In doing so we increase the number of training samples by the factor of 18 resulting in 39024 samples. This dataset is further referred to as ”aug39k”.

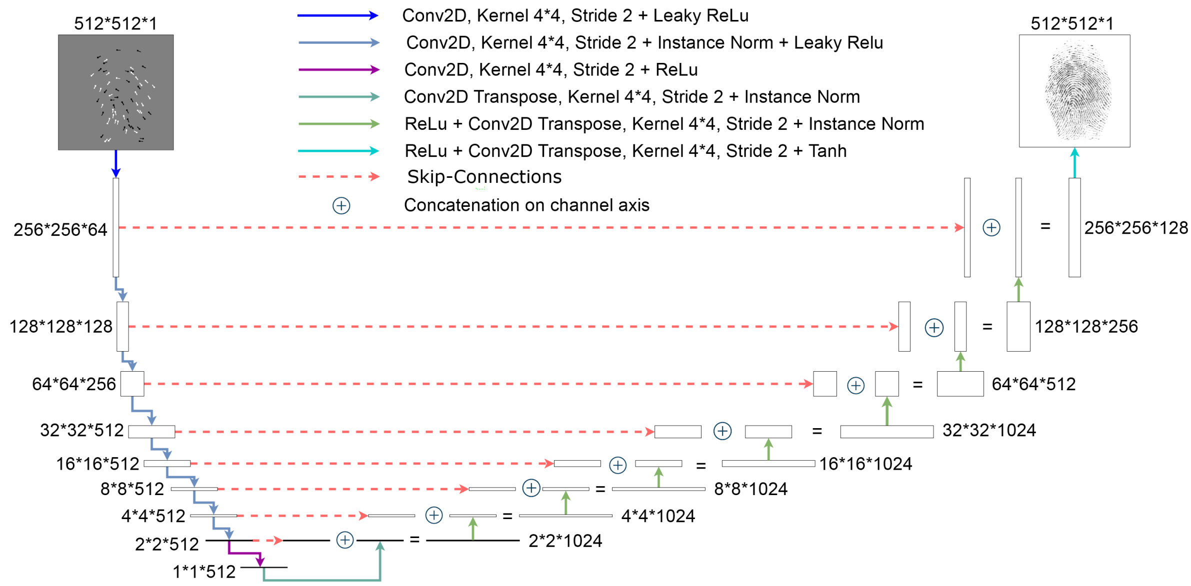

Figure 2: Generator architecture.

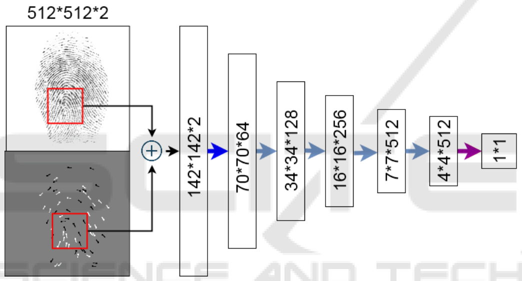

Figure 3: Discriminator architecture - single patch classification; for color encoding of layer transforms see Figure 2.

Figure 4: CrossMatch Verifier 300 fingerprints (top row) vs. our StyleGAN2-ada generated fingerprints (bottom row).

Synthetic Dataset Generation. In order to check whether training of a reliable pix2pix model can be done solely based on synthetic fingerprints, we train the StyleGAN2-ada network (Karras et al. 2020) from scratch based on 408 samples from the Neurotechnology CrossMatch dataset padded to 512x512 pixels with the built-in augmentation. Then we apply the StyleGAN2-ada generator to create 50000 random fingerprints based on the seeds from 1 to 50000. The truncation value has been set to 0.5. This dataset is further referred to as ”syn50k”.

Due to the low number of unique identities in the training dataset, the synthetic samples lack diversity and it is not assured that no identity leakage happens in regard to the training data. However, subjectively, the visual quality of synthetic samples is very high making them almost indistinguishable from real samples. Figure 4 shows several examples of real fingerprints from the Neurotechnology CrossMatch dataset together with synthetic fingerprints generated by our StyleGAN2-ada model.

4 IMPLEMENTATION

The pix2pix network used in our study is cloned from: https://github.com/junyanz/pytorch-CycleGAN-and-pix2pix/ The architectures of generator and discriminator networks are modified to fit our concept as presented in 3.2. Training is performed using the desktop PC with the AMD Ryzen 9 3950X 16-Core 3.5 GHz CPU and 128 GB RAM with two Nvidia Titan RTX GPUs with 24GB VRAM each.

Training Hyperparameters. Aiming at making our generative models comparable to each other we use the same learning rate of 0.002 and train the networks for 60 epochs plus 60 epochs with a learning rate decay. After training, we have realized that non of the final models outperforms the earlier model snapshots. Hence, we have picked the model snapshots after 15, 30 and 55 training epochs for the evaluation to check whether more epochs produce better visual results or lead to a better reconstruction. We first trained the models with batch normalization (batch size of 64) which resulted in noisy fingerprint patterns with a lot of noise especially on image margins which should contain white pixels only. As suggested in (Ulyanov et al. 2016) batch normalization is replaced by instance normalization. It helps to avoid noise but sometimes has a negative effect on a realism of ridge lines. All fingerprint images in which no single minutiae has been detected were excluded from the training.

Resulting Generative Models. After several rounds of training we have ended up with four models all producing visually convincing fingerprint images:

- aug39k_DL, DL = Directed Line
- aug39k_PM, PM = Pointing Minutiae
- syn50k_DL
- syn50k_PM

The first two models have been trained with the augmented CrossMatch dataset (aug39k) with minutiae encoded first by directed lines and then by pointing minutiae. The other two models have been trained with the StyleGAN2-ada generated dataset (syn50k) with minutiae also encoded by directed lines and pointing minutiae. Here, we train no models with minutiae encoded by gray squares because this encoding scheme has been demonstrated to underperform directed line encoding (Makrushin et al. 2022) and our preliminary training results have also confirmed it. After paper publication all our models together with generated synthetic fingerprints will be made public at https://gitti.cs.uni-magdeburg.de/Andrey/gensynth

Figure 5: Anguli (left) vs. URU (right) fingerprint.

5 EVALUATION

5.1 Test Datasets

The two test datasets used for evaluation are completely detached from the training datasets. Each test dataset contains 880 samples.

The first dataset has been created using the open source tool Anguli (Ansari 2011). With this dataset, we expect that a minutiae extraction tool make no errors. Hence, the fingerprint reconstruction performance should be seen as idealistic.

The second dataset is the DB2 A+B dataset from the Third International Fingerprint Verification Competition (FVC2004) which contains real fingerprints collected using a URU 4500 scanner. In contrast to Anguli fingerprints, URU fingerprints are very challenging for any minutiae extractor. Moreover, the fingerprints from URU scanners are dramatically differ from those of CrossMatch scanners used for training of reconstruction models. Figure 5 shows an Anguli vs a URU sample.

5.2 Metrics

The ***realistic appearance*** of reconstructed fingerprints is evaluated using NFIQ2 scores (https://www.nist.gov/services-resources/software/nfiq-2). Although NFIQ2 is designed to predict the utility of a fingerprint meaning its effectiveness for a user authentication process, NFIQ2 is known to correlate well with the visual quality and therefore can be seen as an indicator of realistic appearance. The scores span from 0 to 100 with higher values for higher utility. The scores higher than 35 indicate good fingerprints just as higher than 45 perfect ones. The scores lower than 6 indicate useless patterns.

The ***fingerprint reconstruction success*** is measured by the ratio of fingerprint pairs (target vs. reconstructed) whose matching scores exceed a certain threshold in all tested fingerprint pairs. This measure is identical to the True Acceptance Rate (TAR) of a fingerprint matcher. Following the state-of-the-art studies, we calculate Type1 TAR - matching the reconstructed fingerprint against the finger impression from which the minutiae are extracted. Calculation of Type2 TAR (matching the reconstructed fingerprint against a different finger impression to that from which the minutiae are extracted) will be addressed in future work. Fingerprint matching scores are similarity scores from 0 to infinity produced by the VeriFinger SDK v12.0. The matching algorithm behind VeriFinger is proprietary, but is known to mostly rely on minutiae. The decision threshold is an inherent parameter of a biometric matcher. It is defined based on the required security level of a biometric system which in turn is defined by expected False Accept Rate (FAR) of a matcher. The common levels for FAR are 0.1%, 0.01% and 0.001%, the lower the more secure. The decision thresholds of VeriFinger for those FAR are 36, 48 and 60 correspondingly.

5.3 Results

Realistic Appearance. Figure 6 shows the distributions of NFIQ2 scores. In the first row, the minutiae maps are derived from the Anguli dataset and in the second row from the FVC2004 DB2 A+B dataset. The left column represents models trained with the aug39k dataset and the right column models trained with the syn50k dataset. The NFIQ2 scores of original images are taken as reference. We compare model snapshots after 15, 30 and 55 training epochs.

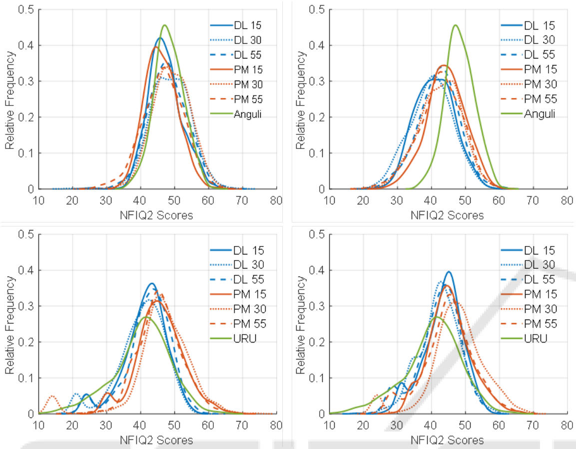

Figure 6: Distributions of NFIQ2 scores for Anguli (top row) and URU fingerprints (bottom row). The left column - aug39k models, right column - syn50k models.

Our main observation is that the visual quality of reconstructed fingerprints rather depends on training samples than on samples from which minutiae have been extracted. Indeed, NFIQ2 scores of original Anguli samples are on average higher than that of reconstructed samples no matter which model has been used. In contrast, NFIQ2 scores of URU samples are significantly lower than that of reconstructed samples for all models.

In bottom diagrams the URU distributions have tails towards lower NFIQ2 scores indicating the presence of several low quality samples in the dataset. For such samples minutiae cannot be reliably extracted leading to incomplete or messed up patterns in reconstructed samples which explains the second peak in reconstructed fingerprint distributions in the area of low NFIQ2 values.

Models with PM encoding in comparison to models with DL encoding seem to produce on average fingerprints with slightly higher NFIQ2 scores except for the aug39k models tested on the Anguli dataset.

From diagrams, no clear conclusion can be drawn which number of training epochs lead to the best visual quality. For instance, with URU test samples and PM encoding, models trained with 30 epochs show the best results. With URU test samples and DL encoding, the best aug39k model is obtained after 55 training epochs.

Table 1: Fingerprint reconstruction success (in %).

			Anguli fingerprints			URU fingerprints		
			Type1 TAR @ FAR of					
Enc	DB	Ep	**0.1%**	**0.01%**	**0.001%**	**0.1%**	**0.01%**	**0.001%**
DL	aug39k	15	**100.00**	**100.00**	99.77	87.84	82.61	76.47
		30	**100.00**	99.77	99.20	83.29	75.11	65.90
		55	99.43	98.52	97.50	79.09	71.81	59.31
	syn50k	15	97.38	97.63	86.47	78.86	71.36	59.20
		30	92.50	84.88	70.56	68.52	55.79	42.84
		55	93.18	86.25	74.31	72.38	62.15	48.18
PM	aug39k	15	**100.00**	**100.00**	**100.00**	**95.45**	**95.00**	**93.52**
		30	**100.00**	**100.00**	**100.00**	95.11	94.31	93.29
		55	99.88	99.43	98.86	93.52	91.36	88.86
	syn50k	15	99.88	99.88	99.77	94.88	94.43	92.95
		30	99.88	99.88	99.65	94.77	93.18	91.59
		55	99.65	98.97	98.52	93.29	90.56	87.38

Fingerprint Reconstruction Success. Table 1 shows the results of fingerprint reconstruction with the idealistic Anguli images (upper bound of reconstruction rates) as well as with URU fingerprints from the FVC2004 DB2 A+B dataset (realistic reconstruction performance). The URU fingerprints for which the VeriFinger minutiae extractor fails to find even a single minutiae are excluded from the experiment as useless. Our observations regarding the reconstruction rates can be summarized as follows:

- All models trained with aug39k are better than their counterparts trained with syn50k.
- PM encoding outperforms DL.
- Model snapshots after 15 training epochs have the best reconstruction performance.
- For PM encoding, the difference between 15 epochs and 30 epochs is almost negligible, while with 55 epochs there is a considerable performance loss.
- For DL encoding, the aug39k snapshot after 15 training epochs is better than that after 30 epochs which is in turn better than that after 55 epochs, but unexpectedly the syn50k snapshot after 15 epochs is better than that after 55 epochs which is in turn better than that after 30 epochs. This applies for both test datasets Anguli and FVC2004 DB2 A+B.

Our most important finding is that with PM encoding the performance drop between aug39k and syn50k is in most cases lower than 1% and in no cases higher than 1,7%. It indicates that StyleGAN2-ada fingerprints can be perfectly used for training pix2pix models aiming at translating minutiae maps to fingerprint images. Figure 7 shows a reconstruction example with both models aug39k and syn50k. The 15 epoch snapshots are utilized. Examples with 30 and 55 epoch snapshots can be found on our website. The images show that our models perform a style transfer i.e. the appearance of resulting fingerprints is similar to those captured with a CrossMatch sensor.

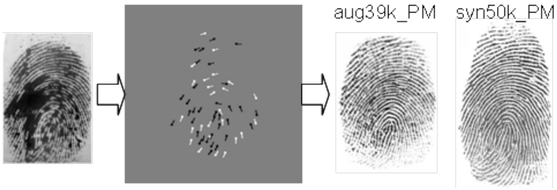

Figure 7: Reconstruction example of a URU fingerprint.

Although the ridge patterns in reconstructed samples are not exactly the same as in target fingerprints, the minutiae co-allocation is reproduced accurately enough to enable matching with the source of minutiae. Hence, we state that pix2pix in conjunction with PM or DL encoding is a valid approach for fingerprint reconstruction from minutiae. We have also shown that the pix2pix architecture is scalable to larger images and training with 512x512 pixel images can be done within a reasonable time frame.

6 CONCLUSION

Reconstruction of realistic fingerprints from minutiae is an important step towards controlled generation of high-quality datasets of synthetic fingerprints. Since, the minutiae co-allocation defines the fingerprint's identity, reconstruction from pseudo-random minutiae maps ensures anonymity and diversity of resulting patterns and enables synthesis of mated fingerprints. This paper introduces and compares four pix2pix models trained with fingerprint images of 512x512 pixels at fingerprint-native resolution from real and synthetic datasets with two types of minutiae encoding. Our experiments show that a pix2pix network is a valid solution to the reconstruction problem with a scalable architecture enabling training with 512x512 pixel images, that reconstructed ridge patterns appear realistic, that pointing minutiae encoding is superior to directed line encoding, that an augmented dataset of 39k real fingerprints used for training is superior to a dataset of 50k synthetic fingerprints, but if pointing minutiae encoding is applied, the difference in reconstruction performances between real and synthetic training data is lower than 1.7%. Future work will be devoted to compilation of a large-scale synthetic fingerprint dataset appropriate for evaluation of fingerprint matching algorithms.

ACKNOWLEDGEMENTS

This research has been funded in part by the Deutsche Forschungsgemeinschaft (DFG) through the research project GENSYNTH under the number 421860227.

REFERENCES

Ansari, A. H. (2011). *Generation and storage of large synthetic fingerprint database*. M.E. Thesis, Indian Institute of Science Bangalore.

Bahmani, K., Plesh, R., Johnson, P., Schuckers, S., and Swyka, T. (2021). High fidelity fingerprint generation: Quality, uniqueness, and privacy. In *Proc. ICIP'21*, pages 3018–3022.

Bouzaglo, R. and Keller, Y. (2022). Synthesis and reconstruction of fingerprints using generative adversarial networks. *CoRR*, abs/2201.06164.

Cao, K. and Jain, A. K. (2015). Learning fingerprint reconstruction: From minutiae to image. *IEEE TIFS*, 10:104–117.

Cappelli, R. (2009). SFinGe. In Li, S. Z. and Jain, A., editors, *Encyclopedia of Biometrics*, pages 1169–1176. Springer US, Boston, MA.

Cappelli, R., Maio, D., Lumini, A., and Maltoni, D. (2007). Fingerprint image reconstruction from standard templates. *IEEE PAMI*, 29:1489–1503.

Feng, J. and Jain, A. (2009). FM model based fingerprint reconstruction from minutiae template. In *Proc. ICB'09*, pages 544–553.

Isola, P., Zhu, J.-Y., Zhou, T., and Efros, A. A. (2017). Image-to-image translation with conditional adversarial networks. In *Proc. CVPR'17*, pages 5967–5976.

Karras, T., Aittala, M., Hellsten, J., Laine, S., Lehtinen, J., and Aila, T. (2020). Training generative adversarial networks with limited data. *CoRR*, abs/2006.06676.

Karras, T., Laine, S., and Aila, T. (2018). A style-based generator architecture for generative adversarial networks. *CoRR*, abs/1812.04948.

Karras, T., Laine, S., Aittala, M., Hellsten, J., Lehtinen, J., and Aila, T. (2019). Analyzing and improving the image quality of StyleGAN. *CoRR*, abs/1912.04958.

Kim, H., Cui, X., Kim, M.-G., and Nguyen, T.-H.-B. (2019). Reconstruction of fingerprints from minutiae using conditional adversarial networks. In *Proc. IWDW'18*, pages 353–362.

Li, S. and Kot, A. C. (2012). An improved scheme for full fingerprint reconstruction. *IEEE TIFS*, 7(6):1906–1912.

Makrushin, A., Kauba, C., Kirchgasser, S., Seidlitz, S., Kraetzer, C., Uhl, A., and Dittmann, J. (2021). General requirements on synthetic fingerprint images for biometric authentication and forensic investigations. In *Proc. IH&MMSec'21*, page 93–104.

Makrushin, A., Mannam, V. S., B.N, M. R., and Dittmann, J. (2022). Data-driven reconstruction of fingerprints from minutiae maps. In *Proc. MMSP'22*.

Mistry, V., Engelsma, J. J., and Jain, A. K. (2020). Fingerprint synthesis: Search with 100 million prints. *CoRR*, abs/1912.07195.

Ronneberger, O., Fischer, P., and Brox, T. (2015). U-Net: Convolutional networks for biomedical image segmentation. *CoRR*, abs/1505.04597.

Ross, A., Shah, J., and Jain, A. K. (2007). From template to image: Reconstructing fingerprints from minutiae points. *IEEE PAMI*, 29:544–60.

Seidlitz, S., Jürgens, K., Makrushin, A., Kraetzer, C., and Dittmann, J. (2021). Generation of privacy-friendly datasets of latent fingerprint images using generative adversarial networks. In *Proc. VISIGRAPP'21, Vol.4: VISAPP*, pages 345–352.

Sherlock, B. and Monro, D. (1993). A model for interpreting fingerprint topology. *Pattern Recognition*, 26(7):1047–1055.

Ulyanov, D., Vedaldi, A., and Lempitsky, V. (2016). Instance normalization: The missing ingredient for fast stylization. *CoRR*, abs/1607.08022.

Wang, T.-C., Liu, M.-Y., Zhu, J.-Y., Tao, A., Kautz, J., and Catanzaro, B. (2018). High-resolution image synthesis and semantic manipulation with conditional GANs. In *Proc. CVPR'18*.

Wijewardena, K. P., Grosz, S. A., Cao, K., and Jain, A. K. (2022). Fingerprint template invertibility: Minutiae vs. deep templates. *CoRR*, abs/2205.03809.